

ACCEPTED MANUSCRIPT • OPEN ACCESS

Evaluation of a micro ionization chamber for dosimetric measurements in image-guided preclinical irradiation platforms

To cite this article before publication: Ileana Silvestre Patallo *et al* 2021 *Phys. Med. Biol.* in press <https://doi.org/10.1088/1361-6560/ac3b35>

Manuscript version: Accepted Manuscript

Accepted Manuscript is “the version of the article accepted for publication including all changes made as a result of the peer review process, and which may also include the addition to the article by IOP Publishing of a header, an article ID, a cover sheet and/or an ‘Accepted Manuscript’ watermark, but excluding any other editing, typesetting or other changes made by IOP Publishing and/or its licensors”

This Accepted Manuscript is © 2021 The Author(s). Published by IOP Publishing Ltd..

As the Version of Record of this article is going to be / has been published on a gold open access basis under a CC BY 3.0 licence, this Accepted Manuscript is available for reuse under a CC BY 3.0 licence immediately.

Everyone is permitted to use all or part of the original content in this article, provided that they adhere to all the terms of the licence <https://creativecommons.org/licenses/by/3.0>

Although reasonable endeavours have been taken to obtain all necessary permissions from third parties to include their copyrighted content within this article, their full citation and copyright line may not be present in this Accepted Manuscript version. Before using any content from this article, please refer to the Version of Record on IOPscience once published for full citation and copyright details, as permissions may be required. All third party content is fully copyright protected and is not published on a gold open access basis under a CC BY licence, unless that is specifically stated in the figure caption in the Version of Record.

View the [article online](#) for updates and enhancements.

Evaluation of a micro ionization chamber for dosimetric measurements in image-guided preclinical irradiation platforms.

Authors: Ileana Silvestre Patallo^{1,2}, Rebecca Carter², David Maughan¹, Andrew Nisbet³, Giuseppe Schettino^{1,4}, Anna Subiel¹

¹National Physical Laboratory, Medical, Marine & Nuclear Department, Medical Radiation Physics and Science Groups, Teddington, UK

²University College London, Cancer Institute, London, UK

³University College London, Department of Medical Physics & Biomedical Engineering, London, UK

⁴University of Surrey, Physics, Faculty of Engineering and Physical Sciences. Guildford, Surrey, UK

Abstract

Image-guided small animal irradiation platforms deliver small radiation fields in the medium energy x-ray range. Commissioning of such platforms, followed by dosimetric verification of treatment planning, are mostly performed with radiochromic film. There is a need for independent measurement methods, traceable to primary standards, with the added advantage of immediacy in obtaining results. This investigation characterizes a small volume ionization chamber in medium energy x-rays for reference dosimetry in preclinical irradiation research platforms.

The detector was exposed to a set of reference x-ray beams (0.5 to 4 mm Cu HVL). Leakage, reproducibility, linearity, response to detector's orientation, dose rate, and energy dependence were determined for a 3D PinPoint ionization chamber (PTW 31022). Polarity and ion recombination were also studied. Absorbed doses at 2 cm depth were compared, derived either by applying the experimentally determined cross-calibration coefficient at a typical small animal radiation platform "user's" quality (0.84 mm Cu HVL) or by interpolation from air kerma calibration coefficients in a set of reference beam qualities.

In the range of reference x-ray beams, correction for ion recombination was less than 0.1%. The largest polarity correction was 1.4% (for 4 mm Cu HVL). Calibration and correction factors were experimentally determined. Measurements of absorbed dose with the PTW 31022, in conditions different from reference were successfully compared to measurements with a secondary standard ionization chamber. The implementation of an End-to-End test for delivery of image-targeted small field plans resulted in differences smaller than 3% between measured and treatment planning calculated doses.

The investigation of the properties and response of a PTW 31022 small volume ionization chamber in medium energy x-rays and small fields can contribute to improve measurement uncertainties evaluation for reference and relative dosimetry of small fields delivered by preclinical irradiators while maintaining the traceability chain to primary standards.

Keywords: dosimetry, small fields, detectors, small animal image-guided radiotherapy

1. Introduction

Well-designed preclinical research and reliable preclinical data are essential to the translatability of results into clinical trials. There are a significant number of examples of preclinical studies involving irradiation of cells and small animal models, with direct impact in supporting radiotherapy clinical trials and particularly those contributing to the generalization of personalized targeted therapeutic approaches (Dreyfuss *et al* 2021), (Sotiropoulos *et al* 2021), (Benci *et al* 2016). Dosimetric evaluation of irradiation devices in the kilovoltage range, delivering clinical radiotherapy treatments, is well-documented by several standard dosimetry protocols or codes of practice (CoPs): AAPM TG-61 (Ma *et al* 2001), IAEA TRS-398 and TRS-277 (IAEA 2006, IAEA 1987) and IPEMB (Klevenhagen *et al* 1996). A comprehensive comparison of the data used by different CoP has also been published (Peixoto and Andreo 2000). Recommendations for dosimetry in conditions of preclinical irradiations are limited or totally absent in those documents.

The majority of preclinical irradiations are conducted in purpose-designed irradiators with radiation beams in the medium energy x-ray range. Differing from conventional (clinical) kilovoltage radiotherapy devices, preclinical irradiators are designed as fully integrated self-shielded cabinets. This leads to challenges associated with maintaining traceability of dosimetry validations, i.e. the impossibility to strictly follow the recommendations from CoPs for measurements of reference dose, due to the lack of physical space to recreate full backscatter settings and differences in surrounding scattering conditions. Some recent efforts towards standardization (Chen *et al* 2019), (Subiel *et al* 2020) aimed to address the influence of lack of backscatter conditions on dosimetry in preclinical x-ray units. At the same time, AAPM TG-319 is working on recommendations for dosimetry in radiobiology, that better reflect experimental conditions in preclinical x-ray conventional cabinets (AAPM 2021). The current lack of accuracy and harmonization in dosimetry evaluations is compromising the required robustness in the comparison of findings published by various preclinical research groups (Draeger *et al* 2020), (Coleman *et al* 2016).

To add to the challenge, in the last two decades, researchers have seen a surge in highly sophisticated preclinical irradiation systems that mimic clinical linear accelerators. Image-guided small animal radiation platforms (IGSARP), such as SARRP (Xstrahl) and SmART+ (Precision X-Ray), offer the possibility to precisely replicate radiotherapy treatment techniques while testing novel treatment approaches. With similar scatter conditions, the major differences with respect to the conventional cabinets are: (1) the possibility to target tumours based on pre-treatment acquired images, (2) calculation of treatment times and dose distributions using a bespoke treatment planning system (TPS), and also, and most distinctively, (3) the capability to irradiate very specific and small regions of interest (ROI) with the use of very small-collimated beams. Those small fields (down to 0.5 mm) represent another significant challenge in the pathway towards accurate dosimetry verification of dose delivered by IGSARP. While dosimetry of small fields in the megavoltage x-ray range (linacs and gamma-knife units) has generated large interest in the medical physics community (Palmans *et al* 2018), it is more difficult to find calculated or measured published data specifically related to devices used for preclinical research in the medium-energy x-ray range (Wang *et al* 2018).

For Xstrahl's SARRP devices, the process of commissioning the TPS Muriplan is solely based on GafchromicTM EBT3 films' (Ashland, New Jersey, USA) dose distributions, traceable to the film calibration with a medium volume ionization chamber in a large (open) field, that is not considered as part of the TPS input data. In order to validate the TPS commissioning process, some research groups have implemented Monte Carlo (MC) modelling tools (Tryggstad *et al* 2009), (Ghita *et al* 2017). Scientists from the University of Maryland have developed an online verification method based on the images acquired by an electronic portal imaging device (EPID) (Anvari *et al* 2020). Others have suggested the use of phantoms capable of accommodating EBT3 films in different orientations (Biglin *et al* 2019). The

use of alanine as a reference detector in a mouse-like phantom, has also been reported by our group (Silvestre Patallo *et al* 2020). The latter demonstrated the need for an independent verification method for the TPS commissioning, after finding larger than 10 % discrepancies between Xstrahl SARRP Muriplan calculated and measured dose, delivered to a ROI in the brain with 10 mm × 10 mm field.

Few institutions working with IGSARP have the resources to implement either MC modelling or EPID based verification tools. The disadvantage of using films and alanine for reference dosimetry and TPS verification is that both detectors need additional post-processing and therefore the results of the comparison are not immediately available.

Dose traceability for the small fields delivered by preclinical devices would benefit from a similar strategy as the one recommended by the IAEA TRS-483 CoP (IAEA 2017) and recently adopted by the update of the IPEM code of practice on reference dosimetry for megavoltage radiotherapy devices (Eaton *et al* 2020). TRS-483 formalism is based on the introduction of an intermediate calibration field in the form of a static *machine specific reference* (msr) or a field nominated as a *plan class specific reference* (pcsr) which, by definition, are closer to specific reference and clinical fields delivered by the radiotherapy devices. In our approach, we considered the introduction of the 10 mm × 10 mm field as a msr for preclinical image-guided devices, specifically for SARRP.

Measurements in the 10 mm × 10 mm field will require a small volume ionization chamber (IC) with stability of the response to some of the beam parameters that could influence the measurement outcome: linearity, energy dependence, dose rate variation, angular response, ion recombination and polarity effects, among others. There will be differences in the implementation, as currently, calibrations in the megavoltage range are performed in terms of dose to water, while in the kilovoltage range, the most common approach by calibration laboratories is to calibrate IC against a primary standard free-air ionization chamber (FAC), and to release certificates in terms of air-kerma calibration coefficients (ARPANSA 2021), (NPL 2021), (BIPM 2021), (NIST Radiation Physics Division 2017).

We evaluated the effects influencing the response of a small volume (3D PinPoint) ionization chamber in medium energy x-rays with the aim of implementing a methodology that could improve the traceability of the measurement chain in IGSARPs. A calibration of the chamber against NPL's primary standard FAC, in a set of reference medium energy x-rays (0.5 to 4 mm Cu HVL) was performed. Subsequently, and to allow for measurements at certain depth in water, a cross-calibration against a secondary standard NE2611 ionization chamber, lead to the experimental determination of the PTW 31022 chamber's correction factor. Measurements, to validate the calibration and correction factors, were performed at the "user's" beam quality (HVL). Finally, a small water-equivalent phantom, accommodating the PTW 31022 ionization chamber was used in an End-to-End test to verify the dose calculated by the TPS.

2. Materials and methods

2.1 PTW 31022 chamber characterization. Irradiation facility and measurement procedures.

The detector investigated was the PTW 3D PinPoint ionization chamber type 31022. It is a vented cylindrical, waterproof and fully guarded IC. It has a nominal sensitive volume of 0.016 cm³ and 99.98 % pure Al central electrode. Other characteristics of the design are described by the manufacturer (PTW Freiburg 2020). Only one detector (S/N 151987) was secured for the experimental work.

A set of four reference medium energy x-ray qualities (expressed in terms of half value layer: HVL) from the 300 kV therapy level facility at NPL was used for the characterization (see Table 1). The x-ray source has an inherent filtration of 0.3 mm aluminium equivalent plus 4.8 mm of PMMA.

Table 1. Therapy level (medium energy X-rays) reference qualities.

Nominal generating potential (kV)	Additional Filtration (mm Sn+mm Cu+mm Al)	HVL (mm Cu)
135	0 + 0.27 + 1.2	0.50
180	0 + 0.54 + 1.0	1.00
220	0 + 1.40 + 0.9	2.00
280	1.5 + 0.26 + 1.0	4.00

Measurements described in this section were performed in the *in-air* setup, with the same procedure as the one used for air kerma calibrations at NPL: chamber fixed in the carriage system with its reference point (on the central axis at the centre of the cavity volume) aligned to the centre of the 7 cm diameter radiation field and the chamber's alignment mark facing the beam. The position of the chamber's reference point (RP) at the centre of the beam was verified with the facility's alignment telescope. A precision micrometer (Mitutoyo 100-2100 mm Tubular Inside Micrometer, 139-177) was used to precisely position the chamber's RP at the same distance from the source as the FAC defining plane. In this orientation, the axis of rotation defined by the central electrode is perpendicular to the centre of the beam. A transmission monitor was used to correct for any variations in the x-ray tube output. When not specifically mentioned to be different, the nominal tube operating current was 10 mA. Under those conditions, the nominal air kerma rate (AKR) is 0.1 Gy/min.

Each final reported value of current is calculated by sampling and averaging 100 independent values of current, acquired with a Keithley 6514 electrometer (S/N 1046588). If not otherwise stated, the working voltage applied to the PTW 31022 chamber was 300 V with negative polarity, which leads to the collection of negative ions. The average current is corrected for any leakage effect, and for temperature (t) and pressure (p) variations, measured by a calibrated thermistor (EPCOS B57861S0302F040, NTC, 3 kohm) placed in the proximity of the IC sensitive volume and a GE Druck DPI 142 barometer (S/N 2644308) placed in the control area. This procedure and the FAC are more extensively described in Kelly (2007). All instruments used during the characterization measurements are regularly calibrated under UKAS-accredited calibration services.

Table 2 summarises each of the *in-air* and *in-phantom* setups. Only the elements with significant impact in the determination of correction factors affecting the response of the chamber and/or dose measurements (i.e. field size, amount of backscatter, etc.) are specified. Pictures of three of the experimental setups are shown in Figure 1.

Table 2 Experimental setups used for the characterization of the PTW 31022 ionization chamber in the medium energy x-rays

	Facility/ HVL (mm Cu)	Field size ^a (cm)	SDD ^b (cm)	Chamber reference point depth (cm)	SSD ^c (cm)	Phantom thickness (cm)	Backscatter material thickness (cm)
<i>in-air</i>		7.0	75	N/A	N/A	N/A	N/A
<i>in-phantom</i> 1	300 kV	7.0	75	2.0	73	6.0	4.0
<i>in-phantom</i> 2 ^d	NPL/Table 1	7.0	75	2.0	73	30	28.0
<i>in-phantom</i> 3		7.0	75	1.0	74	29	28.0
<i>in-phantom</i> 4	UCL (CI)	13.0	35	2.0	33	6.0 ^e	4.0
<i>in-phantom</i> 5	SARRP/0.84	1.0	35	2.0	33	6.0	4.0

^a Field diameter (300 kV NPL facility). Equivalent diameter (UCL (CI) SARRP)

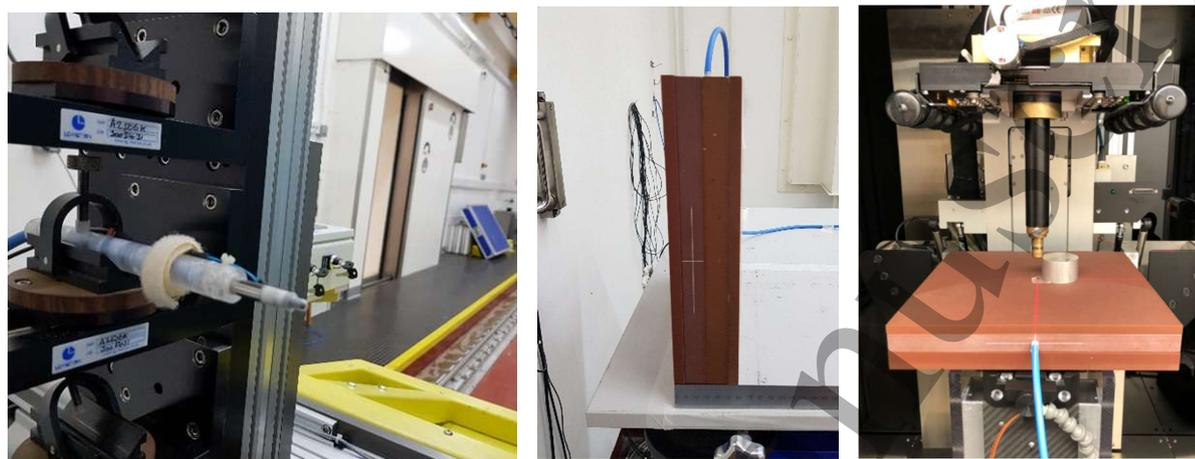
^b SDD: Source Detector Distance (to the position of detector's reference point, the geometrical centre of the chamber)

^c SSD: Source Surface Distance (to the front face of the WT1 phantom)

^d Setup used for chamber cross-calibration at medium energy x-rays reference qualities

^c Including 1 cm from the PMMA calibration platform

For *in-phantom* setups, measurements were performed in a slab phantom of Bart's WT1 solid water (Phoenix Dosimetry Ltd n.d.). WT1 material has been employed before in pre-clinical orthovoltage x-ray work (Soultanidis *et al* 2019) and is very similar in composition to the solid water recommended in the Xstrahl internal commissioning report (Hill *et al* 2005).



(a)

(b)

(c)

Figure 1 Example of the setups used during experiments with the PTW 31022 chamber a) *in-air* setup, b) *in-phantom 1*, c) *in-phantom 5*

2.1.1 Reproducibility, pre- and post-irradiation leakage, linearity, dose rate and directional response

Repeatability was assessed for all beam qualities by recording ten independent values of current measured by the PTW 31022 chamber positioned at the centre of the beam. Measurements were reproduced on the subsequent day after re-establishing the source to the chamber's reference point (RP) distance and verifying its position in the centre of the beam.

Each reported value of pre- and post-irradiation leakage was determined by sampling and averaging 50 readings of current. Post-irradiation leakage was measured 20 seconds after the irradiation was stopped by the closure of the shutter. To investigate the magnitude of the leakage, seven independent repeats of current measurements were acquired for each of the four referred beam qualities (Table 1).

To evaluate the linearity of the chamber response, the average of three corrected measurements of ionization current were recorded at four nominal tube currents: 5, 10, 13 and 15 mA. Stability with air kerma rate variations in the range between 0.05 and 20 Gy/min (as determined with the FAC) was established by comparing the ratios of PTW 31022 readings against monitor chamber readings at different air kerma rate to the ratio at the nominal AKR, for each of the qualities evaluated.

Finally, for the directional response, a SARRP cone beam computed tomography (CBCT) of the PTW 31022 was performed to identify any defects in the chamber construction. Subsequently, at the NPL facility, the chamber was placed with the alignment mark positioned perpendicular to the beam. By keeping the chamber reference point at the centre of the beam, the chamber was carefully rotated along its rotation axis (defined by the central electrode) to two other different positions, separated by 120 degrees. Corrected ionization current was recorded three times at each position.

Linearity, dose rate and directional response were evaluated only for two of the reference qualities: 0.5 and 1 mm of Cu HVL.

2.1.2 Polarity effects on the PTW 31022 chamber's response.

The working operating polarizing voltage for the PTW 31022 chamber was -300 volts (polarity yielding negative charge). Polarity correction was determined in two different settings. The first included measurements *in-air* with the same configuration and methodology as previously described in section 2.1, using the Keithley 6514 electrometer.

The second setup (*in-phantom 1*) involved the use of a field electrometer, in this case a PTW Unidos (S/N 0091¹). Instead of current, a series of three measurements of charge, accumulated during 60 s (corrected for p and t and fluctuations of the x-ray tube) were recorded for each relevant polarizing voltage. Conditions of the reference dose measurements performed in preclinical image-guided irradiators were mimicked. This involved positioning of the ionization chamber at 2 cm depth, with a total thickness of 6 cm (4 cm of backscatter from the centre of the chamber). The source to the chamber centre was kept at 75 cm (SSD = 73 cm). To achieve the desired phantom configuration, a bespoke WT1 plate (30 cm × 30 cm × 2 cm) with an insert for PTW 31022 chamber (PTW-Freiburg 2016), with the centre positioned at 1 cm depth, was used.

In both cases, readings were acquired with the electrometers at the chamber's working operating voltage (300 V) and both polarizations, to collect negative and positive charge. The variation of the polarity correction for selecting a lower operating voltage (200 and 100 V) was also investigated.

Corrections for polarity effects (k_{pol}) in all (four) medium energy x-ray reference beam qualities were calculated according to equation 6 from the AAPM TG-61 CoP (Ma *et al* 2001).

2.1.3 Ion recombination effects on the PTW 31022 chamber's response

For a continuous source of radiation and for the most commonly recommended ionization chambers for reference dosimetry, the two-voltage analysis (TVA) method (Boag and Currant 1980) is adequate to quantify the magnitude of the ion recombination (k_s):

$$k_s(V_1) = \frac{(V_1/V_2)^2 - 1}{(V_1/V_2)^2 - (M_1/M_2)} \quad (1)$$

where M_1 and M_2 are the collected charge (current) at polarizing voltages V_1 and V_2 , respectively. The equation is valid for pairs of voltages where $V_2/V_1 \leq 0.5$, where V_1 is the working operating voltage (-300 V).

Any presence of initial recombination would require a modification to equation (1) (Zankowski and Podgorsak 1998). Previous published research (Miller *et al* 2016, Hyun *et al* 2017, Derikum 2007 and Palmans *et al* 2010), refers to the presence of both effects for microchambers in high energy x-rays beams. However, no studies have been published for microchambers in the medium energy x-ray range. That lead us to investigate the response of the chamber with the Jaffé plot, reported to be more robust than the two-voltage method (McEwen 2010).

¹ Independently of the ionization chamber (PTW 31022, PTW 30012 or NE2611), the PTW Unidos electrometer (S/N 0091) was used in all the experiments referring to charge measurements.

With measurements of current (*in-air* configuration) or charge (*in-phantom I*) for a set of voltages (negative polarity): 50, 100, 150, 200, 250 and 300 V, ion recombination correction was determined by extrapolating the inverse of the measured signal ($1/M$) to the infinite value of voltage (i.e. $1/V = 0$).

The presence of initial recombination was evaluated by comparing k_s obtained from Jaffé plots and the TVA method.

To evaluate the response of the chamber at different polarizing voltages, saturation curves were obtained by normalizing measured values of current (charge) at the selected values of voltage (for both, negative and positive polarity) to the readings at -300 V and +300 V, respectively. A graph of the inverse value of voltage versus the inverse of positive and negative measured signals (averaged over all beam qualities) was also plotted. Inverse of measured signals were normalized to the inverse of the saturation current (charge) at the working polarizing voltage -300 V (Jaffé plot of normalized current).

2.1.4 PTW 31022 free in air calibration in medium energy x-rays and energy dependence evaluation.

To evaluate the energy dependence of the PTW 31022 ionization chamber, a direct calibration in terms of air kerma against the NPL primary standard (FAC) was performed for the reference medium energy x-ray beam qualities (Table 1).

For each beam quality, the following calibration sequence was used: measurements of current with the primary standard FAC, alternating with the PTW 31022 and a repeat of the primary standard measurements. Ratios of FAC to monitor and PTW 31022 to monitor currents were corrected for leakage, pressure, and temperature. The calibration coefficient (N_K) in Gy/C was determined as the ratio of the primary standard to the PTW 31022 chamber response, multiplied by the primary standard sensitivity (in terms of Gy/C) for the particular x-ray quality. To verify the stability of the chamber's performance, the calibration was repeated at least three times in each of five different calibration campaigns, between 2019 and 2020.

The energy dependence of the response of the PTW 31022 chamber was evaluated by comparison to the response of the secondary standard IC NE2611 (S/N 134). The authors of two studies that previously used the same methodology (Li *et al* 1997) and (Hill *et al* 2009) defined a so named relative detector response (RDR) at a particular beam quality (HVL) as:

$$\text{RDR}(HVL_x)_{PTW31022} = \frac{N_k(HVL_x)_{NE2611} \times M(HVL_x)_{NE2611}}{M(HVL_x)_{PTW31022}} \quad (2)$$

where $N_k(HVL_x)_{NE2611}$ is the air kerma calibration coefficient for the 2611 ionization chamber, $M(HVL_x)_{NE2611}$, and $M(HVL_x)_{PTW31022}$ are in air (corrected) readings of current for the NE2611 and the PTW 31022 chambers, respectively. RDRs at different reference beam qualities were normalized to the response of the chamber in the highest quality beam (i.e. 4 mm Cu HVL).

2.2 Experimental determination of chamber's correction factor $k_{ch,31022}$.

For users with interest in evaluating dose at certain depth instead of at the surface of the phantom, which is the case for targeted irradiations in IGSARP devices, CoPs recommend applying the *in-phantom* method for determination of absorbed dose to water at 2 cm depth. For that purpose, equations such as the one presented by the IPEMB code of practice (Klevenhagen *et al* 1996), can be followed:

$$D_{w,z=2} = MN_K k_{ch} \left[\left(\frac{\mu_{en}}{\rho} \right)_{w/air} \right]_{z=2,0} \quad (3)$$

where $D_{w,z=2}$ is the dose to water (Gy) at the position of the chamber centre at depth of 2 cm in water (or water equivalent phantom), M is the measurement system's readings corrected for t and p , N_K is the chamber calibration coefficient, $\left[\left(\bar{\mu}_{en}/\rho\right)_{w/air}\right]_{z=2,\phi}$ is the mass energy absorption coefficient ratio, water to air, averaged over the photon spectrum at 2 cm depth of water and field diameter ϕ . Finally, k_{ch} is the correction factor that takes into consideration changes in the response of the ionization chamber that was calibrated in air and is used to perform measurements in water.

One of the challenges for using *in-phantom* methods based on *in-air* calibration is the lack of information on the chamber correction factor, k_{ch} , particularly if the type of ionization chamber used is not listed in reference documents or if there are no published data. That is the case for the PTW 31022 IC.

The intercomparison method of the field instrument (PTW 31022) versus an NE2611 secondary standard ionization chamber, as recommended in the IPEMB CoP was followed to experimentally determine k_{ch} for the small volume detector, in the four reference beam qualities at NPL 300 kV therapy facility (Table 1).

Measurements were performed in WT1 solid water with the total phantom thickness of 30 cm, to allow for full backscatter conditions (*in-phantom 2*). A WT1 slab plate (30 cm \times 30 cm \times 2 cm) with the insert for the NE2611 IC was carefully interchanged with the one for the PTW 31022. A substitution method was used for the measurement of the two recommended series (1 and 2) of ratios of secondary standard (SS) (M_{NE2611}) to field instrument (M_{31022}) readings (corrected for t and p). By equating absorbed dose from equation (3) for both detectors, it was possible to derive a $k_{ch,31022}$ (based on measurements with the SS NE2611 at NPL reference beam qualities), using the following relation:

$$\left[k_{ch,31022}\right]_{NPL (NE2611 \text{ based})} = k_{ch,NE2611} \times (N_{K,NE2611}/N_{K,31022}) \times (M_{NE2611}/M_{31022})_{true} \quad (4)$$

A series of exposures were given to the two chambers (series 1) and the ratio of readings M_{NE2611}/M_{31022} was calculated for each exposure. Afterwards the chambers were interchanged, and the measurements were repeated (series 2). The true ratio (*true*) of the readings was then calculated using equation (2) from the IPMEB CoP (Klevenhagen *et al* 1996):

The cross-calibration approach was also followed at UCL Cancer Institute (CI) SARRP device (x-ray tube operated at 220 kV and 13 mA), further referred as the user's beam quality (HVL = 0.84 mm Cu). The measurements were performed in non-full backscatter conditions, as described in Table 2 under *in - phantom 4*.

Firstly, based on equation (3), dose at 2 cm depth was calculated from measurements with the same NE2611 SS previously used at NPL 300 kV facility. Subsequently, the PTW 31022 was placed under the same measurement conditions and the chamber correction factor, based on measurements with the SS NE2611, at the user's SARRP beam quality, $\left[k'_{ch,31022}\right]_{SARRP (NE2611 \text{ based})}$, was determined. Finally,

dose at 2 cm depth was also measured with a PTW 30012 IC, the UCL CI secondary standard system. Value of k_{ch} for the PTW 30012 chamber type is not listed, neither in the IPEMB nor in the AAPM CoPs. PTW 30012 and NE2571 ICs, however, have very similar dimensions and chamber materials [33], therefore values from Table VIII of the AAPM CoP for the NE2571 were used for dose calculations according to equation (3). This last set of measurements, led to the determination of a second $\left[k'_{ch,31022}\right]_{SARRP (PTW 30012 \text{ based})}$ (chamber correction factor based on measurements with the SS PTW 30012, at the user's SARRP beam quality). Previously determined correction factors in the user's beam quality (by cross-calibration), were compared to the chamber correction factor derived from the

linear interpolation between the factors determined at the two closest NPL reference qualities (0.5 and 1 mm Cu HVL) to the user's quality (0.84 mm Cu HVL), $[k'_{ch,31022}]_{linear-interpolation}$

2.2.1 Validation of experimentally determined correction factors for the PTW 31022.

To validate the experimental determination of the chamber correction factors, measurements of absorbed dose to water were performed at two different depths and scatter conditions. The first set of measurements was performed with *in-phantom 3* configuration. The second set repeated the conditions for *in-phantom 1*, to mimic similar backscatter conditions to the ones used in SARRP devices.

Absorbed dose rate determined with the SS NE2611 and the PTW 31022 were compared for the four reference beam qualities of the NPL 300 kV therapy level facility (listed in Table 1).

2.3 SARRP machine specific reference field (*msr*) formalism.

The dose at 2 cm depth in the presence of the small field, $D_{w,Q,z=2,\phi=1cm}^{f_{msr}(\phi=1cm)}$ at the user's beam quality (Q), can be calculated (as per equation (5)) by multiplying the product of the chamber calibration and correction factors $[N_{K,Q}k_{ch,Q}]$ by the mass energy absorption coefficient ratio, water to air in the smaller 10 mm \times 10 mm field, $\left[\left(\frac{\mu_{en}}{\rho}\right)_{w/air}\right]_{z=2,\phi=1cm}$. To account for any added effects to the chamber's readings (already corrected for t , p and k_{pol}) for measuring in the 10 mm \times 10 mm *msr* field ($M_{\phi=1cm}$), an additional correction factor, $k_Q^{f_{msr}f_{ref}}$ is introduced.

$$D_{w,Q,z=2,\phi=1cm}^{f_{msr}(\phi=1cm)} = M_{\phi=1cm} N_{K,Q} k_{ch,Q} k_Q^{f_{msr}f_{ref}} \left[\left(\frac{\mu_{en}}{\rho}\right)_{w/air}\right]_{z=2,\phi=1cm} \quad (5)$$

The dose at 2 cm depth delivered by the SARRP reference field (13 cm equivalent diameter) can be calculated using equation (6):

$$D_{w,Q,z=2,\phi=13cm}^{f_{ref}(\phi=13cm)} = M_{\phi=13cm} N_{K,Q} k_{ch,Q} \left[\left(\frac{\mu_{en}}{\rho}\right)_{w/air}\right]_{z=2,\phi=13cm} \quad (6)$$

The relative output factor (ROF) is the ratio of dose measured for the 10 mm \times 10 mm field and the reference field. EBT3 film is a choice of detector for small field ROF determination as they do not suffer from volume averaging effect and have relatively low energy dependence in medium energy x-rays (Wang *et al* 2018). Equation (7) formalises ROF by means of measurements with EBT3 film.

$$\frac{D_{w,Q,z=2,\phi=1cm}^{f_{msr}(\phi=1cm)}}{D_{w,Q,z=2,\phi=13cm}^{f_{ref}(\phi=13cm)}} = \frac{\left[\frac{D_{w,z=2cm}^{\phi=1cm}}{D_{w,z=2cm}^{\phi=13cm}}\right]_{film}}{1} = ROF_{film} \quad (7)$$

Two independent sets of EBT3 film (from the same lot #12131901), for calibration and dose determination, were used. Films were scanned in the EPSON Expression 10000XL Pro flat-bed scanner

(Seiko Epson Corporation, Nagano, Japan, S/N 022879) according to our working protocol (Billas *et al* 2019). Films were analysed with the triple channel dosimetry method (Micke *et al* 2011) as implemented by the FilmQAPro software (Ashland ISP Advanced Materials). Values of dose in a 3 mm × 3 mm region of interest (ROI) and its standard deviation (SD), reported by the red channel were recorded for the calculation of the ROF.

The chamber correction factor $k_Q^{fmsrfref}$ can then be determined using the following relation:

$$k_Q^{fmsrfref} = ROF_{film} \times \left[\frac{M_{\phi=13}}{M_{\phi=1cm}} \right] \times \left[\frac{\left[\left(\frac{\mu_{en}}{\rho} \right)_{w/air} \right]_{z=2, \phi=13cm}}{\left[\left(\frac{\mu_{en}}{\rho} \right)_{w/air} \right]_{z=2, \phi=1cm}} \right] \quad (8)$$

Chamber and film measurements described in this section were all performed in WT1, using the setups described as *in-phantom 4* (reference field) and *in-phantom 5* (10 mm × 10 mm field).

2.3.1 End-to-End dosimetry test

An End-to-End test was developed to obtain immediate results of the dose delivered by a preclinical plan, calculated by SARRP TPS Muriplan. A 10 cm × 10 cm × 2 cm WT1 (small) phantom, with the geometric centre of the chamber in the radial direction at 1 cm depth, was purposely designed.

Following the Muriplan TPS treatment planning workflow, the phantom (with the inserted chamber) was fixed to the SARRP robotic couch system, and a CBCT was acquired. Muriplan tissue segmentation algorithm is restricted, and the system is unable to perform calculations when the isocentre is placed in air. To avoid this, a ROI with the dimensions of the WT1 small phantom was created. A segmentation threshold in the water equivalent tissue range was assigned to that structure. A second ROI, with the approximate dimensions of the PTW 31022 sensitive volume, was built to visualize the position of the isocentre and the field edges with respect to the chamber volume.

Two different plans, each with one anterior field, were created. Field sizes were determined by the 10 mm × 10 mm and 5 mm × 5 mm collimators, respectively. The isocentre was placed at the reference point of the PTW 31022. Finally, Muriplan version 2.2.1 was used to calculate treatment time and dose distribution.

Point doses calculated by Muriplan were compared to measurements with the PTW 31022 ionization chamber for both selected field sizes. All measurements of charge described in this section were performed with the PTW Unidos electrometer and corrected for t and p . Dose was calculated based on equation (3).

2.4 Uncertainties

Uncertainty budgets were derived according to the guide to the expression of uncertainty in measurement, from the Joint Committee for Guides in Metrology (JCGM 2008).

Reproducibility, leakage, linearity, dose rate dependence, directional response and polarity and ion recombination effect Type A uncertainties were determined through the standard deviation of the mean (SDOM) of repeated measurements with a coverage factor of 1 ($k=1$). Reported uncertainties consider not only variations under the same conditions but also the repositioning of the measurement setup.

The overall uncertainty on the experimental determination of chamber's calibration (N_K) and correction k_{ch} factors, as well as those associated to the determination of absorbed dose to water in the conditions of the proposed End-to-End test are presented under the relevant **Results** subsections.

3. Results

3.1. Reproducibility, leakage, linearity, dose rate dependence and directional response of the PTW 31022

For all investigated reference beam qualities, repeatability, expressed as the standard deviation of the mean (SDOM) of ten individual measurements of current (in the order of 10^{-13} A), was within 0.05%. The difference between the averaged measured current after reproducing the measurement setup was within 0.3 %.

Averaged pre- and post-irradiation leakage current were both smaller than 7.0 fA. There was no evident correlation between the magnitude of post irradiation leakage and the beam quality. On average (over the four studied qualities), the signal acquired during irradiation was 177 times larger than the leakage. The largest leakage fraction of measured signal was 0.88% (for 0.5 mm Cu HVL beam quality).

Within the range of the x-ray tube current tested (up to 15 mA) and for the two qualities studied (0.5 and 1 mm Cu HVL), the linearity test showed a linear response of the corrected measured current with delivered air kerma (Figure 2).

PTW 31022 versus monitor chamber readings ratio, at different AKR, was within $\pm 0.5\%$ when compared to the ratio at the system's operational AKR (electron beam current 10 mA). The largest difference for the 0.50 mm Cu HVL beam was 0.4%, at the maximum achievable air kerma rate (0.14 Gy/min for 15 mA electron tube current). For the 1.00 mm Cu HVL beam quality, the largest difference was -0.5%, in this case at the minimum considered air kerma rate for this quality (0.07 Gy/min for 5 mA).

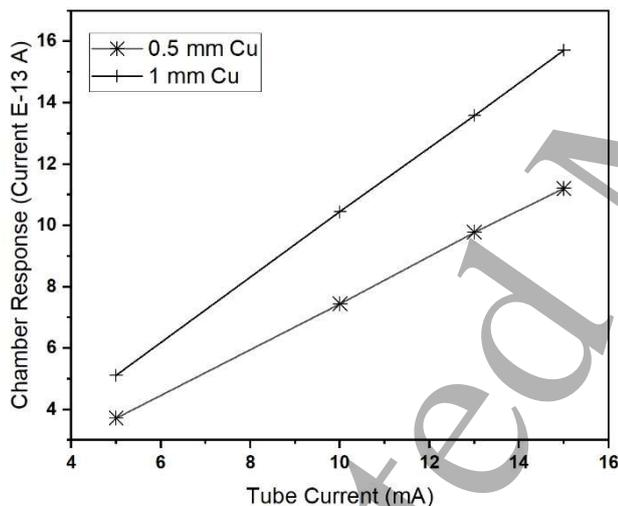


Figure 2 Linearity of the chamber response.

The CBCT image of the PTW 31022 confirmed the straight position of the central electrode as well as no visible defects in the chamber construction. No significant directional dependence was observed. The maximum variation of the response with respect to the one at the recommended position (when the alignment line is perpendicular to the radiation source) was found for the chamber rotated 120 degrees clockwise (towards the x-ray tube) for the two qualities investigated. The differences were 0.18 % and 0.31 % for 0.5 mm and 1 mm Cu, respectively.

3.2 Polarity correction

The polarity of the voltage applied has an effect on the magnitude of the corrected ionization current readings, when measurements with the PTW 31022 chamber are performed in air and connected to the Keithley 6514 electrometer (*in-air* setup). An effect of the same scale was present for charge measurements (also corrected for t and p) with a PTW Unidos electrometer and the chamber at 2 cm depth in a solid water slab phantom setup (*in-phantom 1* setup).

Figure 3 shows polarity correction as a function of the beam quality. Each point represents the average of five independent sets of measurements, all at the operating voltages of 300 V. For three sets, k_{pol} was calculated based on measurements of current; for the remaining two, collected ionization charge was used for the calculations.

The smaller k_{pol} correction (1.010 ± 0.001) was determined for the x-ray beam with the lower quality (0.5 mm Cu HVL), while the larger correction (1.014 ± 0.002) was found for the 2 mm Cu HVL beam quality.

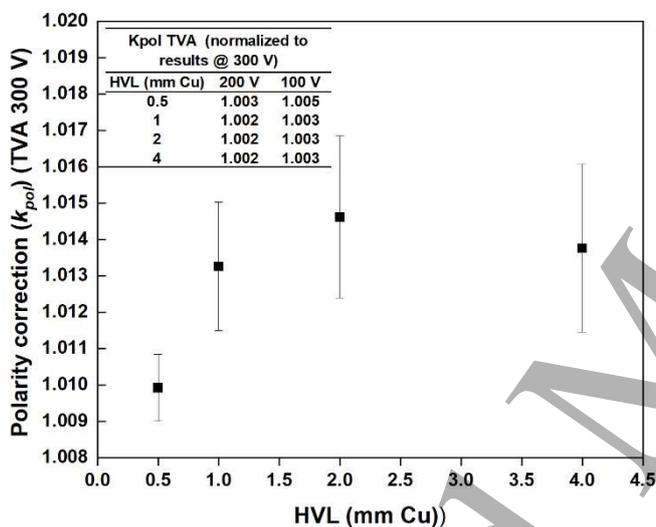


Figure 3 Polarity correction for the PTW 31022 (0.5 to 4 mm Cu HVL, 1 SD error bars). Table embedded: polarity correction at two lower polarizing voltages, normalised to the value at the working polarizing voltage (300 V).

As shown in the embedded table from Figure 3, values of k_{pol} determined by the TVA method at two lower voltages (i.e. 100 and 200 V) are not significantly different from the correction determined at the working polarizing voltage (i.e. 300 V).

3.3 Ion recombination and normalized saturation curves

As expected, ion recombination correction evaluated by the TVA method, for the selected working operating voltage $V_1 = -300$ and $V_2 = -100$ V (collection of negative charge or ionization current) showed no significant energy (HVL) dependence. The averaged ion recombination factor (over the four beam qualities), k_s was found to be 1.001 ± 0.000 .

Ion recombination factor from Jaffe's plots (considering measurements at 50, 100, 150, 200, 250 and 300 V) was found to be (on average over the four beam qualities) 1.001 ± 0.000 .

Within the measurement conditions ($\varnothing 7$ cm field size, a source to detector distance of 75 cm and AKR in the range of 0.1 Gy/min), ion recombination factor (collecting negative ions) determined through Jaffe plot and the two-voltage method analysis, agreed within 0.1%.

Normalized saturation curves for the PTW 31022 (Figure 4 a) show the differences in the response of the chamber depending on the polarity and magnitude of the applied voltage.

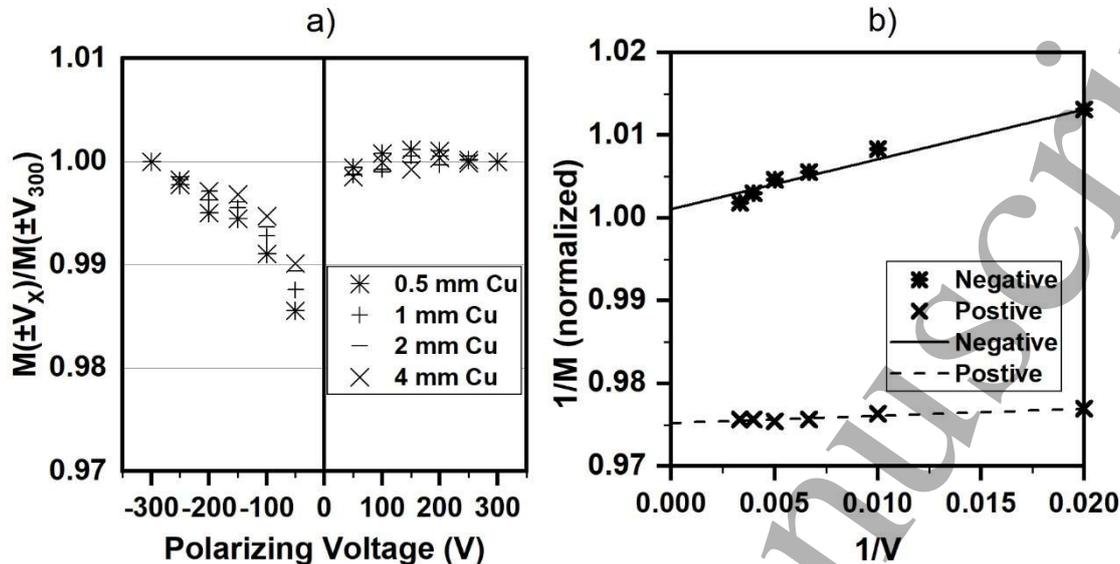


Figure 4 a) Saturation curve for the PTW 31022 IC. Negative and positive measurements are normalized to those at - 300 V and + 300 V respectively. b) Jaffé plots of normalized inversed positive and negative current (charge). At each voltage, $1/M$ is the average of measurements at all four beam qualities, normalized to the inverse of the saturation signal.

For negative applied voltage, the typical behaviour of an ionization chamber is observed, with the signal of the chamber decreasing for lower applied voltages. The effect is evident for all beam qualities, with the larger deviation from unity for the lower (0.5 mm Cu HVL) beam quality ($M_{-50V}/M_{-300V} = 0.984$).

The response of the chamber connected to positive bias voltages (positive charge collection) shows a different behaviour. The average ratio of readings at each positive applied voltage, to the one at the (maximum) positive operating voltage (+300 V) was closer to a constant unity value, for each individual quality. When collecting positive signal, the response of the chamber appears not to be significantly influenced by changes in the magnitude of the applied voltage (in the considered range of voltages).

The uncertainty of the ratios in Figure 4 a), expressed in terms of the standard deviation of the average current (charge) at each of the bias voltage, was estimated to be 0.2 %.

Jaffé plots of normalized signal ($1/M$) in Figure 4 b), showed different gradient and intercepts when collecting negative or positive ions.

3.4 PTW 31022 air kerma calibration in medium energy x-rays. Energy dependence.

Calibrating the PTW 31022 micro ionization chamber did not present particular challenges, compared to what is the routine process for calibration of secondary standard in medium energy x-rays.

Figure 5 presents the derived chamber calibration coefficients, N_K , for each of the beam qualities investigated.

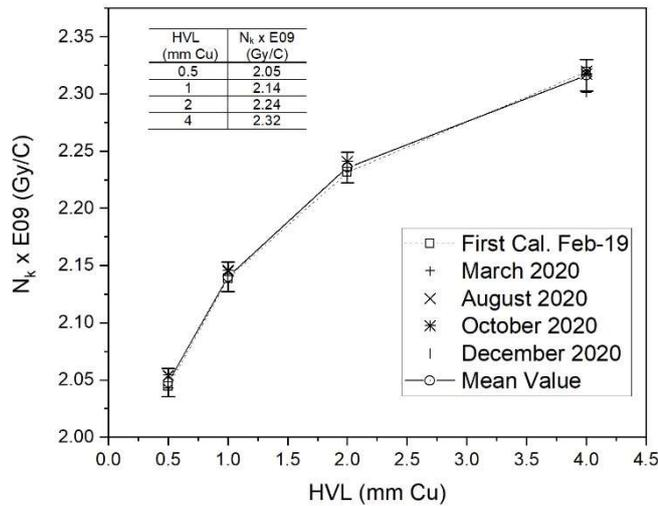


Figure 5. PTW 31022 chamber calibration coefficient N_K for medium energy x-ray qualities (0.5-4 mm Cu HVL).

Values of N_K for a given calibration campaign (averaged over all the repeats) were always within the 0.6 % (represented by the error bars in Figure 5), when compared to the values reported by the previous calibration. The result is considered a good evidence of chamber stability within the period of time where this particular chamber was evaluated. The N_K values in the table within Figure 5 represent the mean N_K of the calibration repetitions for each of the investigated qualities.

The PTW 31022 shows a large energy dependence in the studied range of medium energy x-rays. As an indication, the calculated maximum to minimum N_K ratio was found to be 13.5%. Comparing the PTW 31022 to a secondary standard NE2611 therapy dosimetry chamber, the RDR (normalized at 4 mm Cu HVL) was 0.89, 0.93 and 0.97 for 0.5, 1- and 2-mm Cu HVL, respectively.

For all beam qualities, combined standard uncertainty ($k=1$) of the experimentally determined $N_{K,31022}$ was 1.26 %. In the analysis Table 22 of NPL report 54 (Bass *et al* 2019) was used as reference. The small chamber's volume and the large leakage fraction were considered. Despite having only one chamber, the calibration process was repeated several times through a period of almost two years.

Table 3 Uncertainty budget for determination of air kerma calibration coefficients (N_K). Values are given as one relative standard uncertainty ($k=1$).

Sources of uncertainty	Type A (%)	Type B (%)
Air kerma rate		0.55
Electrometer current calibration (pA/pA')		0.15
Electrometer resolution (pA)		0.03
Ion recombination correction	0.1	
Leakage current (A)	0.5	
Current measurements (A)	0.05	
Temperature (K)	0.02	
Pressure (kPa)	0.04	
Distance from source correction		0.001
Orientation of chamber		0.05
Repeatability	1	
Combined standard uncertainty ($k=1$)		1.26

3.5 Experimentally determined $k_{ch,31022}$ for the PTW 31022 chamber. Validation of the results

The k_{ch} correction factors for the PTW 31022 chamber are presented in Table 4. Values of $k_{ch,2611}$, used here to derive the micro chamber correction factors, are included in the table for reference. Values of the overall chamber correction factor, $P_{Q,cham,2611}$, according to the formalism in AAPM TG-61 are also presented for comparison.

Table 4. Experimentally determined chamber correction factors for a PTW 31022 ionization chamber.

HVL (mm Cu)	$k_{ch,31022}$	$k_{ch,2611}^a$	$P_{Q,cham,2611}^b$
0.5	1.027	1.023	1.019
1	1.008	1.022	1.017
2	1.001	1.020	1.011
4	1.007	1.018	1.003

^a Table 4 in the IPEMB CoP, ^b Table VIII in the AAPM TG-61 CoP

Combined standard uncertainty ($k=1$) of the experimentally determined k_{ch} is 3.24 %. It considers combined uncertainties for all components in Equation (4). Uncertainties for k_{ch} and N_K for the NE2611 chamber (Type B) were taken from section 3.3 in the IPEMB CoP (Klevenhagen *et al* 1996), and the NPL report 54 (Bass *et al* 2019), respectively. For the PTW 31022 chamber calibration coefficient (N_K), the uncertainty was evaluated in this work (Table 3). Type A uncertainties for the ratio of the collected charge between the secondary standard and the 31022 chambers, where determined from the experimental work.

Table 5. Uncertainty budget for determination of chamber correction factor k_{ch} . Values are given as one relative standard uncertainty ($k=1$).

Sources of uncertainty	Type A (%)	Type B (%)
k_{ch} NE2611		3
Calibration Coefficient $N_{K,2611}$		0.37 ^a
Calibration Coefficient $N_{K,31022}$		1.13 ^a
Ratio of collected charge (NE2611/31022)	0.25	
Temperature (K)	0.02	
Pressure (kPa)	0.04	
Combined standard uncertainty ($k=1$)		3.24

^a Due to the high correlation of the two N_K coefficients through the primary standard (FAC), uncertainties related to AKR measurements have been removed from the uncertainty budget evaluation.

Values of absorbed dose rate measured in conditions different to the ones used to determine the PTW 31022 chamber correction factor $k_{ch,31022}$ are summarized in Table 6. Values of dose rate measured with the NE2611 SS ionization chamber, are presented for comparison.

Table 6. Measurements of absorbed dose to water. Validation of the experimental determination of $k_{ch,31022}$.

Setup	HVL (mm Cu)	Dose $\times 10^{-3}$ (Gy/s)		% Δ^a
		PTW 31022	2611	
<i>in-phantom 1</i>	0.5	1.70	1.69	-0.53
	1.0	2.51	2.50	-0.26
	2.0	2.42	2.42	0.09
	4.0	2.30	2.30	0.18
<i>in-phantom 3</i>	0.5	1.93	1.92	-0.61
	1.0	2.79	2.77	-0.60
	2.0	2.65	2.64	-0.19
	4.0	2.48	2.49	0.33

$$^a \% \Delta = 1 - Dose_{PTW31022} / Dose_{2611A}$$

3.5.1 Determination of $k'_{ch,31022}$ by cross-calibration in the user's beam

Measurement of dose rate at 2 cm depth in the conditions of *in-phantom 4* setup at UCL CI SARRP with two different secondary standard systems (PTW 30012 and NE2611 IC) was 3.03 and 3.07 Gy/min, respectively.

The cross-calibration by substitution of the PTW 31022 chamber yielded $[N_K k_{ch}]_{cross-calibra}$ values of 2.132×10^9 Gy/C and 2.160×10^9 Gy/C using the NE2611 and the PTW 30012 ionization chambers, respectively.

From equation (4), $k'_{ch,31022}$ was calculated in the user's beam. Air kerma calibration coefficient for the PTW 31022 was determined by linear interpolation (between 0.5 and 1 mm Cu HVL), from the values reported in Figure 5.

$[k'_{ch,31022}]_{SARRP (PTW 30012 \text{ based})}$ and $[k'_{ch,31022}]_{SARRP (PTW NE2611 \text{ based})}$ were found to be 1.023 ± 0.021 and 1.010 ± 0.020 , respectively. That is respectively, 0.90 % larger and 0.40 % smaller than the value obtained by linear interpolation from the correction factors established at NPL reference qualities 0.5 and 1 mm Cu ($k'_{ch,31022,interpolated} = 1.014 \pm 0.020$). Differences between factors determined by the two different methods and with two different secondary standard chambers (NE2611 and 30012) are all within the experimental uncertainties.

3.6 PTW 31022 chamber response in small field size beams.

ROF for the 10 mm \times 10 mm field, determined with EBT3 film was 0.602. Ratio of corrected charge readings measured with the PTW 31022 chamber, at the reference and the 10 mm \times 10 mm fields was 1.672. The quotient of the mass energy absorption coefficient ratio, water to air over the photon spectrum in the reference and 10 mm \times 10 mm fields was 0.991. Following the formalism described in section 2.3 and employing equation (8), the correction factor $k_Q^{fmsrref}$, accounting for any changes in the response of the chamber different from those already included in the IPEMB formalism for in phantom dose measurements at 2 cm depth, was found to be 0.997 ± 0.012 . The uncertainty for the correction factor was established based on the calculation of the maximum and minimum ROF by evaluating the standard deviation of dose for the two independent sets of films.

3.6.1 End-to-End test measurements with the PTW 31022 chamber in the small WT1 phantom

With the procedure described in section 2.3.1 (using density override for the calculations), the external contour of the phantom was correctly identified by Muriplan. For the isocentre positioned at the centre of the chamber's volume and at 1 cm depth in the phantom, the TPS also correctly calculated the beam SSD (34 cm). The SSD is an important parameter used by the TPS algorithm to calculate isodoses and irradiation time.

For the 10 mm × 10 mm collimator, Muriplan-calculated dose for a 120 s treatment was 4.08 Gy. Whereas, the measured dose with the ionization chamber was 4.18 Gy, giving a 2.48 % dose difference, considering the measured dose as the reference. With the same treatment time, the difference for the 5 mm × 5 mm collimator was 1.91 % (3.90 Gy and 3.98 Gy for the calculated and measured dose, respectively). Future work will include a more comprehensive evaluation of the validity of the use of the PTW 31022 chamber in field sizes smaller than 10 mm × 10 mm.

Table 7 below presents the uncertainties associated with measurements of dose in the conditions relevant to the End-to-End test. Possible variations of water to air mass-energy absorption coefficient ratio and chamber correction factor, because of the deviation from reference conditions (depth and phantom thickness) have not yet been investigated and therefore were not considered in the analysis. Considering the range of the user's beam quality, those uncertainties should not add a significant figure to the quoted value.

Table 7 Uncertainty budget for determination of absorbed dose with the End-to-End test. Values are given as one relative standard uncertainty ($k=1$)

Sources of uncertainty	Type A (%)	Type B (%)
$k_{ch\ 31022}^a$		3.3
Calibration coefficient $N_{K\ 31022}^b$		1.3
mass-energy absorption coefficient ratio, water to air		1.2 ^c (0.3) ^d
Interpolation of quantities of influence for the user's HVL		1.5
Dosimeter readings M	0.2	
Temperature (K)	0.1	
Pressure (kPa)	0.1	
Combined standard uncertainty ($k=1$)	4.0 (3.9)	

^{a,b} Determined as part of our experimental work

^c According to table 1 of the IPEMB CoP ((Klevenhagen et al 1996).

^d According to table 1 from more recently published data for the dosimetry of low- and medium-energy kV x rays (Andreo 2019)

4. Discussion

Despite the importance in accurate delivery of dose in preclinical radiation research, reference dosimetry of small fields in medium energy x-rays (0.5 to 4 mm Cu HVL) has not been the subject of many scientific investigations. Our evaluation of the performance of the PTW 31022 small volume ionization chamber in medium energy x-rays demonstrated its capability as an alternative detector (with the advantage of an immediate result) to films and alanine, for measurements of reference dose in small fields, delivered by image-guided preclinical irradiation platforms.

A characterization of leakage, ion recombination and polarity has been presented, and contributes to the quantitative evaluation of the behaviour of the chamber in reference and users' beam qualities in the medium energy x-ray range. For the combination of PTW 31022 chamber and Keithley 6514 electrometer, the leakage fraction of the measured signal (at air kerma rates between 0.005 and 0.20 Gy/min) was just

below 0.9 % for all investigated beam qualities. That is larger than a leakage fraction of 0.05-0.2 % reported for measurements with similar chambers in water with MV beams (McEwen 2010). Pre- and post- irradiation leakage (on the order of fA) are very similar to those reported by other authors (McEwen 2010),(Le Roy *et al* 2011). The larger relative contribution of leakage to the actual chamber signal (current) needs to be considered within the uncertainties of the determination of the chamber calibration coefficient.

The saturation curve (Figure 4 a) demonstrates that when the chamber is measuring negative current (charge), the PTW 31022 chamber's response is very similar to what have been reported for reference chambers like the NE2571 (Le Roy *et al* 2011) (lower values of ionization current or charge at lower applied voltage). A different behaviour is shown when the chamber is collecting positive charge, with almost no voltage-dependence response observed. Similar voltage-dependent polarity effects of micro ionization chambers have been associated to changes in the ionization chamber collecting volume caused by potential difference between collecting electrodes (Miller *et al* 2016). For chambers of the same type, the effect is potentially specific to each individual chamber. The studied chamber showed a voltage-dependent polarity effect for all the beam qualities. Further investigation should be carried out for other PTW 31022 chambers and preferably for other types of microchambers, including evaluation at different dose rates.

Difference in the intercepts of graphs shown in Figure 4 b), confirms the differences in response of the chamber at different polarizing voltages (section 3.3). Observed differences in the gradient, albeit for a different energy range and pulsed type of beam, have been previously reported for a small volume IBA CC01 ionization chamber (McEwen 2010). Our study of ion recombination with the TVA method, lead to an average value of 1.000 ± 0.000 for the combination $V_1 = +300V, V_2 = +100V$, which was not significantly different from the k_s determined for the negative operational bias voltage ($V_1 = -300V, V_2 = -100V$) yielding 1.001 ± 0.000 . That is a confirmation that differences in the response at different polarizing voltages cannot be attributed to ion recombination processes. Similar to McEwen, we do not have an explanation for the experimental result at this time.

Neither AAPM TG-61 nor IPEMB CoP specify the range of acceptable values for polarity correction for the chambers recommended for reference dosimetry in medium energy x-rays. The value of the polarity correction determined is higher than the 0.4 % specified for reference-class ionization chambers in the addendum to the AAPM TG-51 protocol (for reference dosimetry in high-energy photon beams) (McEwen *et al* 2014). However, the k_{pol} determined for the PTW 31022 ionization chamber was smaller than the 3 %, which is considered to be the limit for a chamber to be suitable for measurements of absolute dose (Andreo *et al* 2005). Moreover, the variation of k_{pol} with energy across the total range of reference medium energy x-rays was 0.45 %, which is slightly lower than the 0.5 % recommended in the same document.

The product $[N_k k_{ch}]$ for the PTW 31022 (S/N 151987) varies 9.8% over the energy range of the reference medium energy x-rays (twice as much as recommended by the IPEMB CoP for reference dosimetry). However, the majority of image-guided preclinical irradiation platforms have a beam quality between 0.5 and 1 mm Cu HVL. For the studied PTW 31022 chamber, the product $[N_k k_{ch}]$ varies less than 2.6 % between those two qualities, that combined with the observed stability of the calibration coefficient over the two years recalibration period (with less than 0.6 % change) leads us to consider the PTW 31022 as a prospective candidate for reference dosimetry in medium energy x-rays, more specifically when small fields are involved.

The validity of the experimental determination of $k_{ch,31022}$ was demonstrated by comparing measurements of absorbed dose to water (in a water equivalent slab phantom) at two different setups with measurements performed with a secondary standard detector. Future work will include Monte Carlo

simulations for the determination of $k_{ch,31022}$ and its comparison with the experimentally determined factors.

We presented a dosimetry chain that includes direct reference dose measurements at the user's beam quality and in the presence of the small fields delivered by image-guided preclinical irradiation platforms. Following the described formalism, it was demonstrated that within the experimental uncertainty, there is no need for an additional correction to the response of the chamber for measurements of absorbed dose to water in SARRP's beam quality and with a small $10\text{ mm} \times 10\text{ mm}$ field size. Our measurements showed that volume averaging effect is not present in the measurements with the PTW 31022 in the $10\text{ mm} \times 10\text{ mm}$ field size. At the same time, differences in beam quality between the larger (open field) and the $10\text{ mm} \times 10\text{ mm}$ field size are already considered by the *in-phantom* method (as presented in the IPEMB CoP) by the selection of the $\left[\left(\bar{\mu}_{en}/\rho \right)_{w/air} \right]_{z=2,0}$ for the measured field (in this case the $10\text{ mm} \times 10\text{ mm}$ field).

The simple End-to-End dosimetry test presented here enabled the comparison of measured versus TPS-calculated dose, in a solid water phantom fixed to the positioning system, while targeting the chamber reference point within the sensitive volume. The size of the PTW 30122 chamber restricts the use of the dosimetry verification test in plans with fields smaller than $5\text{ mm} \times 5\text{ mm}$. However, considering the limitations of the TPS used (Muriplan), for which density override of the chamber cavity was used for the calculations, difference in calculated versus measured dose smaller than 3 % are very encouraging towards achieving a dosimetry measurement methodology for direct and online pre-treatment verification of more complex beam arrangements. Future work will consider the adaptation of a zoomorphic phantom to include the insertion for a small volume ionization chamber.

5. Conclusions

We evaluated the performance of a PTW 31022 micro ionization chamber, in medium energy x-rays. The experimentally determined calibration coefficient and correction factors allow for the chamber to be used for an accurate determination of absorbed dose to water in small fields delivered by image-guided preclinical irradiation platforms that to date are mostly verified off-line, using radiochromic films or alanine.

The possibility of using a small volume ionization chamber for absolute dose measurements in the $10\text{ mm} \times 10\text{ mm}$ field opens an avenue for the cross-calibration of diodes, that could then be used for an independent verification for the TPS commissioning of the smaller fields. The prospect of improving the dosimetry chain with an End-to-End test, similar to those implemented for radiotherapy patient-specific QA, and using a detector with direct traceability to a primary standard for medium energy x-rays, is a step forward in reducing uncertainties for preclinical irradiations. A more robust and reliable dosimetry chain for image-guided preclinical irradiation platforms could contribute to harmonized dosimetry assessments across different institutions and therefore to the reduction of uncertainties in preclinical radiation research.

Acknowledgments

The experimental work performed at UCL CI was supported by the Radiation Research Unit at the Cancer Research UK City of London Centre Award [C7893/A28990]

References

AAPM 2021 Task Group No. 319 - Guidelines for accurate dosimetry in radiation biology experiments (TG319) (https://www.aapm.org/org/structure/?committee_code=TG319)

- 1
2
3
4
5
6 Andreo P. 2019 Data for the dosimetry of low and medium energy kV x-rays *Phys. Med. Biol.* 64(20),
7 5019-37
8
9 Andreo P, Seuntjens J P and Podgorsak E B. 2005 Chapter 9. Calibration of photon and electron beams.
10 In: Podgorsak E B. ed. *Review of Radiation Oncology Physics: A Handbook for Teachers and*
11 *Students*
12
13 Anvari A, Modiri A, Pandita R, Mahmood J and Sawant A. 2020 Online dose delivery verification in small
14 animal image-guided radiotherapy *Med. Phys.* 47(4), 1871–9
15
16 ARPANSA 2021 Medium energy X-rays (MEX) ([https://www.arpansa.gov.au/our-services/testing-and-](https://www.arpansa.gov.au/our-services/testing-and-calibration/calibration/psdl/medium-energy-x-ray)
17 [calibration/calibration/psdl/medium-energy-x-ray](https://www.arpansa.gov.au/our-services/testing-and-calibration/calibration/psdl/medium-energy-x-ray))
18
19 Bass G A, Duane S, Kelly M, Manning J W, Maughan D J, Nutbrown R F, Sander T and Shipley D R. 2019
20 NPL REPORT IR 54. The NPL Air Kerma Primary Standard Free-Air Chamber for medium energy x-
21 rays: summary of factors incorporating ICRU report 90 recommendations. (Teddington)
22 (<https://eprintspublications.npl.co.uk/8504/1/IR54.pdf>)
23
24 Benci J L, Xu B, Qiu Y, Wu T J, Dada H, Twyman-Saint Victor C, Cucolo L, Lee D S M, Pauken K E, Huang A
25 C, Gangadhar T C, Amaravadi R K, Schuchter L M, Feldman M D, Ishwaran H, Vonderheide R H,
26 Maity A, Wherry E J and Minn A J. 2016 Tumor Interferon Signalling Regulates a Multigenic
27 Resistance Program to Immune Checkpoint Blockade *Cell* 167(6), 1540-1554.e12
28
29 Biglin E R, Price G J, Chadwick A L, Aitkenhead A H, Williams K J and Kirkby K J. 2019 Preclinical
30 dosimetry: Exploring the use of small animal phantoms *Radiat. Oncol.* 14(1), 1–10
31
32 Billas I, Bouchard H, Oelfke U and Duane S. 2019 The effect of magnetic field strength on the response
33 of Gafchromic EBT-3 film *Phys. Med. Biol.* 64(6), 06NT03
34
35 BIPM 2021 Primary standard for medium-energy x-radiation
36 (https://www.bipm.org/en/bipm/ionizing/dosimetry/x-ray/medium_energy.html)
37
38 Boag J W and Curren J. 1980 Current collection and ionic recombination in small cylindrical ionization
39 chambers exposed to pulsed radiation *Br. J. Radiol.* 53(629), 471–8
40
41 Chen Q, Molloy J, Izumi T and Sterpin E. 2019 Impact of backscatter material thickness on the depth
42 dose of orthovoltage irradiators for radiobiology research *Phys. Med. Biol.* 64(5), 055001
43
44 Coleman C N, Higgins G S, Brown J M, Baumann M, Kirsch D G, Willers H, Prasanna P G S, Dewhirst M
45 W, Bernhard E J and Ahmed M M. 2016 Improving the predictive value of preclinical studies in
46 support of radiotherapy clinical trials *Clin. Cancer Res.* 22(13), 3138–47
47
48 Derikum K. 2007 Evaluation of different methods for determining the magnitude of initial
49 recombination in ionization chambers. Proceedings of Absorbed Dose and Air Kerma Primary
50 Standards Workshop, LNHB (Paris) (http://www.nucleide.org/ADAKPS_WS/)
51
52
53
54
55
56
57
58
59
60

- 1
2
3
4
5
6 Draeger E, Sawant A, Johnstone C, Koger B, Becker S, Vujaskovic Z, Jackson I L and Poirier Y. 2020 A
7 Dose of Reality: How 20 Years of Incomplete Physics and Dosimetry Reporting in Radiobiology
8 Studies May Have Contributed to the Reproducibility Crisis *Int. J. Radiat. Oncol. Biol. Phys.* **106**(2),
9 243–252
- 10
11
12 Dreyfuss A D, Goia D, Shoniyozov K, Shewale S V., Velalopoulou A, Mazzoni S, Avgousti H, Metzler S D,
13 Bravo P E, Feigenberg S J, Ky B, Verginadis I I and Koumenis C. 2021 A novel mouse model of
14 radiation-induced cardiac injury reveals biological and radiological biomarkers of cardiac
15 dysfunction with potential clinical relevance *Clin. Cancer Res.* **27**(8), 2266–76
- 16
17
18 Eaton D J, Bass G A, Booker P, Byrne J, Duane S, Frame J, Grattan M W D, Thomas R A S, Thorp N and
19 Nisbet A. 2020 IPEM code of practice for high-energy photon therapy dosimetry based on the NPL
20 absorbed dose calibration service *Phys. Med. Biol.* **65**(19), 195006
- 21
22
23 Ghita M, McMahon S J, Thompson H F, McGarry C K and King R. 2017 Small field dosimetry for the small
24 animal radiotherapy research platform (SARRP) *Radiat. Oncol.* **12**(1), 204
- 25
26
27 Hill R, Holloway L and Baldock C. 2005 A dosimetric evaluation of water equivalent phantoms for
28 kilovoltage x-ray beams *Phys. Med. Biol.* **50**(21), N331-44
- 29
30
31 Hill R, Mo Z, Haque M and Baldock C. 2009 An evaluation of ionization chambers for the relative
32 dosimetry of kilovoltage x-ray beams *Med. Phys.* **36**(9), 3971–81
- 33
34
35 Hyun M A, Miller J R, Micka J A and Dewerd L A. 2017 Ion recombination and polarity corrections for
36 small-volume ionization chambers in high-dose-rate, flattening-filter-free pulsed photon beams
37 *Med. Phys.* **44**(2), 618–27
- 38
39
40 INTERNATIONAL ATOMIC ENERGY AGENCY 2006 Absorbed Dose Determination in External Beam
41 Radiotherapy. Technical Report Series 398 (Vienna, Austria)
- 42
43
44 INTERNATIONAL ATOMIC ENERGY AGENCY 1987 Absorbed Dose Determination in Photon and Electron
45 Beams: An International Code of Practice. Technical Report Series 277 (Vienna, Austria)
- 46
47
48 INTERNATIONAL ATOMIC ENERGY AGENCY 2017 Dosimetry of Small Static Fields Used in External Beam
49 Radiotherapy. Technical Report Series No. 483 (Vienna, Austria)
- 50
51
52 JCGM 2008 Evaluation of measurement data - guide to the expression of uncertainty in measurements
53 JCGM100 2008
- 54
55
56 Kelly M. 2007 kV X-Ray Dosimetry at NPL Pract. Course Ref. Dosim. (Course Notes)
57 ([http://resource.npl.co.uk/docs/science_technology/ionising](http://resource.npl.co.uk/docs/science_technology/ionising_radiation/clubs_groups/pcrd/pcrd_sessions.pdf)
58 [radiation/clubs_groups/pcrd/pcrd_sessions.pdf](http://resource.npl.co.uk/docs/science_technology/ionising_radiation/clubs_groups/pcrd/pcrd_sessions.pdf))
- 59
60
61 Klevenhagen S C (Chair), Aukett R J, Harrison R M, Moretti C, Nahum A E and Rosser K E. 1996 The
62 IPEMB code of practice for the determination of absorbed dose for x-rays below 300 kV generating

- potential (0.035 mm Al - 4 mm Cu HVL; 10 - 300 kV generating potential) *Phys. Med. Biol.* **41**(12), 2605–25
- Li X A, Ma C M and Salhani D. 1997 Measurement of percentage depth dose and lateral beam profile for kilovoltage x-ray therapy beams *Phys. Med. Biol.* **42**(12), 2561–2568
- Ma C M, Coffey C W, DeWerd L A, Liu C, Nath R, Seltzer S M and Seuntjens J P. 2001 AAPM protocol for 40-300 kV x-ray beam dosimetry in radiotherapy and radiobiology *Med. Phys.* **28**(6), 868–93
- McEwen M, Dewerd L, Ibbott G, Followill D, Rogers D W O, Seltzer S and Seuntjens J. 2014 Addendum to the AAPM's TG-51 protocol for clinical reference dosimetry of high-energy photon beams *Med. Phys.* **41**(4), 041501
- McEwen M R. 2010 Measurement of ionization chamber absorbed dose kQ factors in megavoltage photon beams *Med. Phys.* **37**(5), 2179–93
- Micke A, Lewis D F and Yu X. 2011 Multichannel film dosimetry with nonuniformity correction *Med. Phys.* **38**(5), 2523–34
- Miller J R, Hooten B D, Micka J A and DeWerd L A. 2016 Polarity effects and apparent ion recombination in microionization chambers *Med. Phys.* **43**(5), 2141–52
- NIST Radiation Physics Division 2017 Calibration of X-Ray Radiation Detectors (<https://www.nist.gov/system/files/documents/2017/02/07/procedure03v420.pdf>)
- NPL 2021 X-ray air kerma and absorbed dose to water calibration (<https://www.npl.co.uk/products-services/radiotherapy-diagnostic/x-ray-air-kerma>)
- Palmans H, Andreo P, Huq M S, Seuntjens J, Christaki K E and Meghzifene A. 2018 Dosimetry of small static fields used in external photon beam radiotherapy: Summary of TRS-483, the IAEA–AAPM international Code of Practice for reference and relative dose determination *Med. Phys.* **45**(11), e1123–45
- Palmans H, Thomas R A S, Duane S, Sterpin E and Vynckier S. 2010 Ion recombination for ionization chamber dosimetry in a helical tomotherapy unit *Med. Phys.* **37**(6), 2876–89
- Peixoto J G P and Andreo P. 2000 Determination of absorbed dose to water in reference conditions for radiotherapy kilovoltage x-rays between 10 and 300 kv: A comparison of the data in the IAEA, IPEMB, DIN and NCS dosimetry protocols *Phys. Med. Biol.* **45**(3), 563–75
- Phoenix Dosimetry Ltd Bart's Solid Water for Electrons and Photons (<https://phoenix-dosimetry.co.uk/wp-content/uploads/2020/01/Barts-Solid-Water-for-Electrons-and-Photons.pdf>)
- PTW-Freiburg 2016 Ionization Chamber PinPoint 3D Type 31022. User Manual
- PTW Freiburg 2020 PTW Detectors Catalog (http://www.ptw.de/online_brochures.html)

- 1
2
3
4
5
6 Le Roy M, De Carlan L, Delaunay F, Donois M, Fournier P, Ostrowsky A, Vouillaume A and Bordy J M.
7 2011 Assessment of small volume ionization chambers as reference dosimeters in high-energy
8 photon beams *Phys. Med. Biol.* **56**(17), 5637–50
9
- 10 Silvestre Patallo I, Subiel A, Westhorpe A, Gouldstone C, Tulk A, Sharma R A and Schettino G. 2020
11 Development and Implementation of an End-To-End Test for Absolute Dose Verification of Small
12 Animal Preclinical Irradiation Research Platforms *Int. J. Radiat. Oncol. Biol. Phys.* **107**(3), 587-596
13
14
- 15 Sotiropoulos M, Brisebard E, Le Dudal M, Jouvion G, Juchaux M, Crépin D, Sebie C, Jourdain L, Labiod
16 D, Lamirault C, Pouzoulet F and Prezado Y. 2021 X-rays minibeam radiation therapy at a
17 conventional irradiator: Pilot evaluation in F98-glioma bearing rats and dose calculations in a
18 human phantom *Clin. Transl. Radiat. Oncol.* **27**, 44–9
19
20
- 21 Soultanidis G, Subiel A, Renard I, Reinhart A M, Green V L, Oelfke U, Archibald S J, Greenman J, Tulk A,
22 Walker A, Schettino G and Cawthorne C J. 2019 Development of an anatomically correct mouse
23 phantom for dosimetry measurement in small animal radiotherapy research *Phys. Med. Biol.*
24 **64**(12), NT02.
25
26
- 27 Subiel A, Silvestre Patallo I, Palmans H, Barry M, Tulk A, Soultanidis G, Greenman J, Green V L,
28 Cawthorne C and Schettino G. 2020 The influence of lack of reference conditions on dosimetry in
29 pre-clinical radiotherapy with medium energy x-ray beams *Phys. Med. Biol.* **65**(8), 5016–37
30
31
- 32 Tryggestad E, Armour M, Iordachita I, Verhaegen F and Wong J W. 2009 A comprehensive system for
33 dosimetric commissioning and Monte Carlo validation for the small animal radiation research
34 platform *Phys. Med. Biol.* **54**(17), 5341–57
35
36
- 37 Wang Y-F, Lin S-C, Na Y H, Black P J and Wu C-S. 2018 Dosimetric verification and commissioning for a
38 small animal image-guided irradiator *Phys. Med. Biol.* **63**(14), 5001–10
39
40
- 41 Zankowski C and Podgorsak E B. 1998 Determination of saturation charge and collection efficiency for
42 ionization chambers in continuous beams *Med. Phys.* **25**(6), 908–15
43
44
45
46
47
48
49
50
51
52
53
54
55
56
57
58
59
60